Comparison of the Extent and Severity of Myocardial Perfusion Defects Measured by CT Coronary Angiography and SPECT Myocardial Perfusion Imaging

Balaji K. Tamarappoo, MD, PhD,* Damini Dey, PhD,*† Ryo Nakazato, MD, PhD,*
Haim Shmilovich, MD,* Thomas Smith, MD,‡ Victor Y. Cheng, MD,*†
Louise E. J. Thomson, MBChB,* Sean W. Hayes, MD,* John D. Friedman, MD,*
Guido Germano, PhD,† Piotr J. Slomka, PhD,† Daniel S. Berman, MD*†

Los Angeles and Davis, California

OBJECTIVES We compared electrocardiogram-gated computed tomography (CT) myocardial perfusion imaging (MPI) based on quantification of the extent and severity of perfusion abnormalities to that measured with single-photon emission computed tomography (SPECT) MPI.

BACKGROUND Contrast-enhanced CT-MPI has been used for the identification of myocardial ischemia.

METHODS We performed CT-MPI during intravenous adenosine infusion in 30 patients with perfusion abnormalities on rest/adenosine stress SPECT-MPI acquired within 60 days (18 stress-rest CT-MPI and 12 stress CT-MPI only). The extent and severity of perfusion defects on SPECT-MPI were assessed on a 5-point scale in a standard 17-segment model, and total perfusion deficit (TPD) was quantified by automated software. The extent and severity of perfusion defects on CT-MPI was visually assessed by 2 observers using the same grading scale and expressed as summed stress score and summed rest score; visually quantified TPD was given by summed stress score/(maximal score of 68) and summed rest score/68. The magnitude of perfusion abnormality on CT-MPI in regions of the myocardium was defined.

RESULTS On a per-segment basis, there was good agreement between CT-MPI and SPECT-MPI with a kappa of 0.71 (p < 0.0001) for detection of stress perfusion abnormalities. Automated TPD on SPECT-MPI was similar to visual TPD from CT-MPI (p = 0.65 stress TPD, and p = 0.12 ischemic TPD stress-rest) with excellent agreement (bias = −0.3 for stress TPD, and bias = 1.2 for ischemic TPD) on Bland-Altman analysis. Software-based quantification of the magnitude of stress perfusion deficit and ischemia on CT-MPI were similar to that for automated TPD measured by SPECT (p = 0.88 stress, and p = 0.48 ischemia), with minimal bias (bias = 0.6, and bias = 1.2).

CONCLUSIONS Stress and reversible myocardial perfusion deficit measured by CT-MPI using a visual semiquantitative approach and a visually guided software-based approach show strong similarity with SPECT-MPI, suggesting that CT-MPI–based assessment of myocardial perfusion defects may be of clinical and prognostic value. (J Am Coll Cardiol Img 2010;3:1010–9) © 2010 by the American College of Cardiology Foundation

Coronary computed tomography angiography (CTA) provides excellent anatomic assessment of the extent and severity of coronary artery disease (CAD) and has high diagnostic accuracy for detection of obstructive CAD (1–4). However, the presence of luminal stenosis on coronary CTA does not reliably predict myocardial ischemia, frequently leading to the use of single-photon emission computed tomography (SPECT) myocardial perfusion imaging (MPI) after coronary CTA (5–7). Adenosine-induced defects in myocardial perfusion can be visualized on computed tomography (CT) by examining the differences in contrast distribution between normal and hypoperfused myocardium (8,9). Initial studies show that adenosine CT-MPI has good diagnostic accuracy for detecting myocardial ischemia when compared to invasive coronary angiography (10–13). The ability of CT-MPI to assess the extent and severity of myocardial ischemia has not been fully explored. To examine the potential of CT-MPI to study both coronary artery stenosis and myocardial perfusion, we compared the extent and severity of myocardial hypoperfusion on CT-MPI during adenosine stress using a semiquantitative, 5-point visual assessment, and the magnitude of myocardial hypoperfusion on CT-MPI to hypoperfusion on SPECT-MPI.

METHODS

Patients and study protocol. Thirty-two consecutive patients with a stress perfusion defect ≥5% of total myocardium or a summed stress score (SSS) ≥4 using a 17-segment American Heart Association scoring model on SPECT-MPI were prospectively enrolled in a research protocol for imaging myocardial perfusion by CT-MPI (Fig. 1). Stress CT-MPI was performed within 60 days of SPECT-MPI, and no patients experienced interval change in clinical status or coronary revascularization. Patients with heart failure, acute coronary syndrome, reactive airway disease, chronic kidney disease, and allergy to iodinated contrast were excluded. One patient with respiratory motion artifacts on CT-MPI and another with artifacts from ventricular premature beats were excluded from analysis. The study was approved by our institutional review board, and all patients provided written informed consent for analysis of their data.

CT-MPI. IMAGE ACQUISITION. The CT-MPI was performed on a SOMATOM Definition dual-source CT scanner (Siemens Medical Solutions, Forchheim, Germany), with a temporal resolution of 83 ms, as described previously (14–16). For stress-CT perfusion, 140 μg/kg/min adenosine was infused through an antecubital vein with continuous electrocardiographic monitoring. At 3 min of adenosine infusion, 80 ml intravenous contrast (Omnipaque or Visipaque, GE Healthcare, Princeton, New Jersey) was injected (5 ml/s), followed by 80 ml saline (5 ml/s) (Fig. 1). Automatic bolus tracking of the arrival of contrast (CT attenuation of 100 Hounsfield units [HU]) in the ascending aorta at the level of the pulmonary artery bifurcation was used to trigger image acquisition with a 6-s delay (15). Electrocardiography-gated scanning from 1 cm below the tracheal bifurcation to the level of the diaphragm was performed in a single breath-hold. Adenosine infusion was stopped immediately upon completion of CT image acquisition. In 5 patients who underwent SPECT-MPI on the same day as the CT-MPI, ^{99m}Tc-sestamibi was injected 2 min after initiation of adenosine infusion; adenosine was continued to complete a 5-min infusion. In 18 patients, rest CT-MPI was also performed 10 min later. For rest CT-MPI, sublingual spray of 0.4 mg nitroglycerin (Sciele Pharma, Alpharetta, Georgia) was administered. Metoprolol was administered intravenously (in 5-mg increments, to a maximum of 30 mg) to achieve a heart rate of <60 beats/min in 12 patients. Scanning parameters for stress and rest included heart rate-dependent pitch (0.2 to 0.45), 330 ms gantry rotation time, 100 or 120 kilovoltage (kVp) tube voltage depending on patient weight and body mass index, and 330 to 350 mAs reference tube current (16). For rest, we used the MIND-OSE protocol with maximum tube current delivered at 70% of the R-R interval, as previously described (16). For stress, maximum tube current was delivered over 40% to 70% of the R-R interval. Effective radiation dose in the patients for combined stress and rest CT-MPI was 18 ± 7.1 mSv, using a factor of 0.014 mSv · mGy^{-1} · cm^{-1} to convert from dose-length product (17).

CT-MPI. IMAGE RECONSTRUCTION. Retrospectively gated reconstruction of raw CT-MPI data at stress was performed at 40% and 70% of the R-R interval using 0.6-mm slice thickness (0.75-mm if body mass index was >35 kg/m²), 0.3-mm slice increment, 250-mm field of view, 512 × 512 matrix, and B26f reconstruction kernel. For visualization of

ABBREVIATIONS AND ACRONYMS

CAD = coronary artery disease

CT = computed tomography

CTA = computed tomography angiography

ECG = electrocardiogram

LV = left ventricle

MPI = myocardial perfusion imaging

SPECT = single-photon emission computed tomography

SRS = summed rest score

SSS = summed stress score
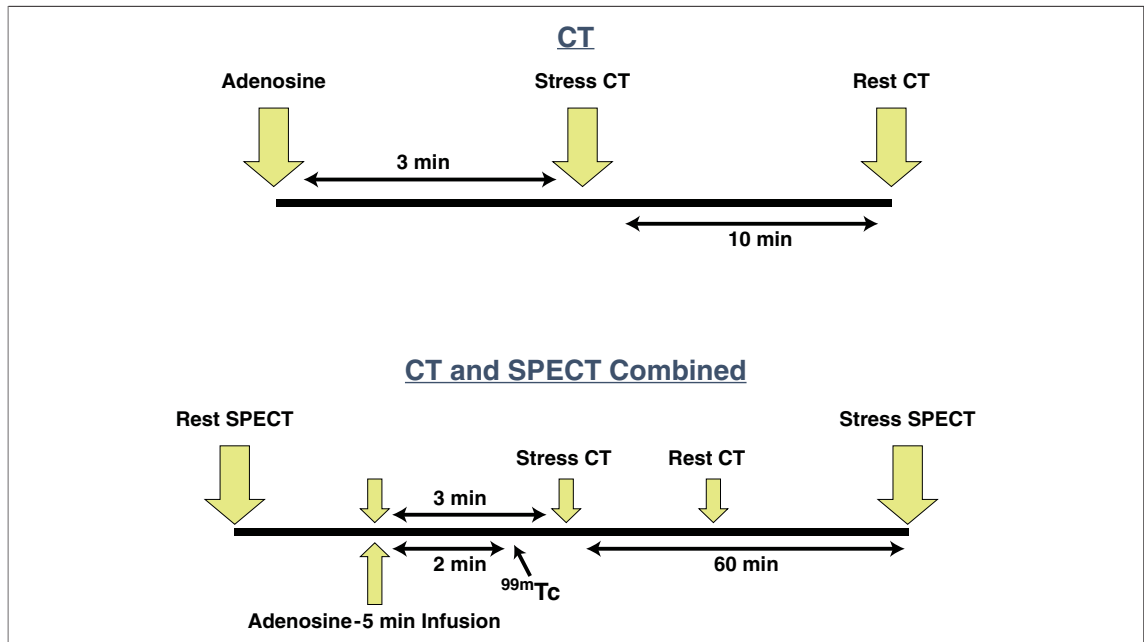
TPD = total perfusion deficit

Figure 1. Schematic Representation of CT-MPI Protocol

(Top) Adenosine stress computed tomography (CT) myocardial perfusion imaging (MPI) was performed in 24 patients known to have a myocardial perfusion defect on a prior single-photon emission computed tomography (SPECT) MPI study using the protocol shown; and of these patients, 16 underwent stress and rest CT-MPI. **(Bottom)** In 6 patients with known myocardial perfusion abnormalities returning for a repeat SPECT-MPI, both stress SPECT-MPI and stress CT-MPI were performed on the same day, and 2 of these patients underwent both stress and rest CT-MPI.

myocardium with stress-induced changes in perfusion, images were reconstructed with 1-mm slice thickness, 0.5-mm slice increment, 250-mm field of view, 512 × 512 matrix, and a B10f reconstruction kernel (12). The use of a B10f kernel has been demonstrated to provide optimal visualization of perfusion defects in previous studies (12,18). Reconstructed data were transferred to a Siemens workstation (Leonardo, Siemens Medical Solutions). For each dataset, oblique image manipulation was used to create true short-axis, 10-mm thick multiplanar reformat images of the left ventricle (LV).

Interpretation of myocardial perfusion on CT-MPI. Display window and level settings were 200 to 300 HU and 100 to 150 HU, respectively (12). Regions of myocardium that exhibited significantly reduced CT attenuation as a result of decreased contrast distribution were considered to have abnormal perfusion. The attenuation of normal myocardium in each patient was used as an internal reference to which hypoperfused myocardium was visually compared to assess the relative severity of hypoperfusion. All CT-MPI studies were assessed by 2 independent experienced readers who scored each individual segment using a standard 17-segment

model with consensual assignment of final scores. True perfusion defects were differentiated from potential artifacts (due to beam hardening and motion) by examining myocardial contrast distribution in both systolic and diastolic phases, requiring reduced attenuation in both sets of images for abnormality (12,18). The magnitude of perfusion defect on CT-MPI was assessed by 2 methods.

Visual assessment of perfusion deficit on CT-MPI. The extent and severity of perfusion defect in each segment was graded on a 0 to 4 scale (0 = uniform CT attenuation equal to normal myocardium; 1 = mildly reduced attenuation encompassing <50% of the myocardium; 2 = moderately reduced attenuation comprising <50% of the myocardium; 3 = moderately reduced attenuation in 50% to 75% of the myocardium or severely reduced attenuation in <50% of the myocardium; and 4 = moderate reduction in attenuation in >75% of the myocardium or severely reduced attenuation in 50% to 75% of the myocardium). Severe reduction of CT attenuation was defined as complete absence of opacification of the myocardium and attenuation that was reduced by >2 SD from the mean attenuation of normal myocardium. Moderately reduced CT attenuation was defined as partial loss of opacification

of myocardium with CT attenuation that was reduced by >1 SD and <2 SD from the mean CT attenuation of normal myocardium (Fig. 2). The CT-MPI–based SSS and SRS were derived by adding the scores assigned to each individual segment from stress and rest. A summed difference score was given by the difference between SSS and SRS. A visually assessed total perfusion deficit (TPD) for CT-MPI was derived by dividing CT-MPI SSS by 68 (which represents the sum of the maximum scores that could be assigned to each of the 17 segments), an approach previously applied to SPECT-MPI (19).

Software-based quantification of perfusion deficit on CT-MPI. In addition to the visual assessment of TPD by CT-MPI, we also quantified the magnitude of myocardial hypoperfusion with commercially available software (Volume, Siemens Medical Solutions) on a Siemens workstation (Leonardo, Siemens Medical Solutions) by manually tracing the regions of hypoperfusion on axial CT-MPI images. Regions of abnormal perfusion were identified by consensual visual assessment by 2 expert readers. Each observer traced a region of interest defining the hypoperfused area on axial slices. The CT attenuation of normally perfused myocardium was defined by measuring the attenuation at multiple points in transverse coronal and saggital views; a mean and SD for normal attenuation was derived from these measurements. Using this mean value and a lower threshold of 0 HU as the attenuation range, the total volume of abnormal myocardium within all the axial regions of interest was computed by the software. In cases of disagreement between readers, myocardium was considered hypoperfused if CT attenuation was >1 SD below the mean attenuation measured in normal myocardium. The volume of myocardium with stress perfusion defect was divided by volume of the entire LV myocardium to quantify the magnitude of stress perfusion deficit. The magnitude of ischemia was given by the difference in the magnitude of perfusion deficit quantified on stress and rest CT-MPI.

Exercise and adenosine stress SPECT-MPI. PROTOCOLS. Patients were instructed to discontinue beta-blockers and calcium antagonists 48 h before, and nitrates 24 h before testing. Rest perfusion images were acquired 10 min after infusion of 7 to 9 mCi of ^{99m}Tc-sestamibi or 3 to 4.5 mCi of [201]Tl (based on body weight). Stress testing was performed with a symptom-limited Bruce treadmill exercise protocol or vasodilator challenge, as described previously (20). At near-maximal exercise, ^{99m}Tc-sestamibi (32 to 40 mCi based on patient weight) was injected intravenously, after which treadmill exercise was continued at maximal workload for 1 min and at 1 stage lower for an additional 2 min whenever possible. The ^{99m}Tc-sestamibi MPI acquisition was started 15 to 30 min after radiopharmaceutical injection. For vasodilator stress, adenosine was infused at 140 μg/kg/min for 5 min; in ambulatory patients, a low-level treadmill exercise was performed during adenosine infusion (21). At the end of the second min, ^{99m}Tc-sestamibi (32 to 40 mCi) was injected, and myocardial imaging was started approximately 60 min later (22). A 12-lead electrocardiogram was monitored continuously during stress testing.

SPECT-MPI. ACQUISITION AND RECONSTRUCTION PROTOCOLS. The SPECT images were acquired with a 2-detector gamma camera (ADAC Forte, Philips Medical Systems, Cleveland, Ohio; or E-Cam, Siemens Medical Solutions). High-resolution collimators were used, and acquisition consisted of 64 projections over a 180° orbit, with 64 projections at 25 s/projection for supine ^{99m}Tc acquisition, followed immediately by 15 s/projection for prone ^{99m}Tc acquisition (21,22). Rest ^{201}Tl acquisition was performed at 35 s/projection in supine position. No attenuation or scatter correction was applied. After iterative reconstruction (12
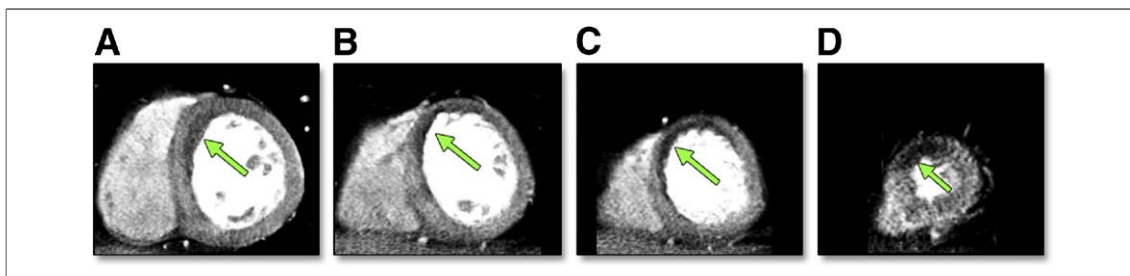
Figure 2. Stress CT-MPI Representing Visual Segmental Scores of 1 to 4 in a Single Patient

(A to D) Perfusion defects, indicated by **green arrows**, on adenosine stress CT-MPI in different segments (basal anteroseptum, mid-anteroseptum, mid-distal septum, and distal anterior wall and septum) in 1 patient. The extent and severity of stress perfusion defect in the anteroseptum in (A to C) was given scores of 1, 2, and 3, respectively. The extent and severity of perfusion defect in the anterior wall in (D) was assigned a score of 4. Abbreviations as in Figure 1.

Table 1. Patients and Study Characteristics

Characteristic	Value
n	30
Male	24
Body mass index	26 ± 3.4
Patients with prior PCI or CABG	17
Duration in days between SPECT-MPI and CT-MPI	9.2 ± 13.9
Patients with stress and rest CT-MPI	18
Patients with only stress CT-MPI	12
Heart rate range during stress CT-MPI	48–119
Maximum heart rate during stress CT-MPI	84.6 ± 17
Heart rate range during rest CT-MPI	39–78
Maximum heart rate during rest CT-MPI	56.2 ± 7.7
Patients with exercise stress during SPECT-MPI	11
Patients with vasodilator stress during SPECT-MPI	19
Effective radiation dose stress and rest CT-MPI, mSv	19.9 ± 6.7 (n = 18)
Effective radiation dose stress CT-MPI alone, mSv	15.7 ± 7.4 (n = 12)
Effective radiation dose in patients without CABG, mSv	15.9 ± 6.3 (n = 20)
Effective radiation dose SPECT-MPI, ^{99m}Tc/^{99m}Tc, mSv	13.1 ± 0.5 (n = 25)
Effective radiation dose SPECT-MPI, ^{201}Tl/^{99m}Tc, mSv	21.8 ± 3.0 (n = 5)

Body mass index, heart rate, and effective radiation dose are expressed as mean ± SD.
CABG = coronary artery bypass graft surgery; CT = computed tomography; MPI = myocardial perfusion imaging; PCI = percutaneous coronary intervention; SPECT = single-photon emission computed tomography.

iterations) with Butterworth pre-filtering (cutoff, 0.66 cycle/pixel for supine ^{99m}Tc, 0.55 cycle/pixel for prone ^{99m}Tc; order 5), short-axis images were automatically generated (23).

Automated quantification of SPECT-MPI. Perfusion defect assessment on SPECT-MPI was performed using an automated quantification of TPD that was calculated as the percentage of the total surface area of the LV below the predefined uniform average deviation threshold weighted on a pixel-by-pixel basis by the severity of perfusion on a scale from 0 to 4 using QPS software (Cedars Sinai, Los Angeles, California) (24,25). This 0 to 4 grading scale is similar to what is used for visual assessment of SPECT-MPI using a 17-segment model. Automated fusion software was used for matching perfusion defects on CT-MPI to perfusion defects on SPECT (26).

Statistical analysis. Continuous variables, including TPD, and the magnitude of perfusion deficit were expressed as mean ± SD. Normally distributed continuous variables were compared using a paired *t* test. The presence of perfusion defects by SPECT-MPI or CT-MPI was considered a categorical variable. Per-segment–based comparison of abnormal segments by CT-MPI and SPECT-MPI was expressed as sensitivity and specificity, using SPECT-MPI as reference. Kappa estimates were used to evaluate the agreement between the 2 independent CT-MPI readers and between CT-MPI and SPECT-MPI in identification of hypoperfused myocardial segments (27). Agreement between automated TPD by SPECT-MPI, visually derived TPD by CT-MPI, and semiautomated quantification of the magnitude of perfusion deficit by SPECT-MPI, were assessed by Bland-Altman analysis (28).

RESULTS

Patient characteristics. Of the 30 patients (24 male) included in the analysis, 12 underwent SPECT-MPI and a stress CT-MPI scan, and 18 underwent SPECT-MPI, stress CT-MPI, and rest CT-MPI (Table 1). The first 12 patients underwent only stress CT-MPI and served as the test cohort for optimization of scanning conditions.

SPECT-MPI and CT-MPI findings. All patients had at least 1 segment with abnormal myocardial perfusion during stress with SPECT-MPI and CT-MPI. Twenty-three (77%) had perfusion abnormalities at rest and stress with a TPD ≥5 on SPECT-MPI (Table 2), and 7 patients had SPECT-MPI abnormalities only during stress. Of 18 patients who underwent stress and rest CT-MPI, 8 had perfusion defects only during stress (reversible defect), and 10 had perfusion abnormalities at stress and rest (reversible and fixed defects). The CT perfusion at rest was normal, whereas SPECT detected a small perfusion defect (TPD = 5) at rest in only 1 patient. We were unable to distinguish between reversible and fixed perfusion defects in patients who underwent stress CT-MPI in the absence of rest CT-MPI; however, in 4 patients, wall thinning of the hypoperfused myocardium suggested that part of the perfusion defect could represent old infarction. Stress TPD on SPECT-MPI ranged from 5 to 30 (15 ± 9.7), and visual TPD on stress CT-MPI ranged from 4 to 29 (14.6 ± 7.2). There was excellent agreement between 2 expert independent readers in identifying regions of myocardium with stress perfusion abnormalities using CT-MPI, with a kappa of 0.88 and a 95% confidence interval of 0.81 to 0.95, p < 0.0001.

CT-MPI and SPECT-MPI identification of stress-induced myocardial hypoperfusion. There was good agreement between CT-MPI and SPECT-MPI in identifying segments with abnormal myocardial perfusion (segmental perfusion score >1), with a kappa of 0.71 and 95% confidence interval of 0.65 to 0.78, p < 0.0001. There was good correspondence of segments with abnormal perfusion on SPECT and

Table 2. Comparison of SPECT-MPI and CT-MPI

	SPECT	CT-MPI	p Value
Patients with stress perfusion defects only	7	8	
Patients with stress and rest perfusion defects	23	10	
Stress TPD (n = 30)	15 ± 9.7	14.6 ± 7.2	0.65
Rest TPD (n = 18)	3.2 ± 3.5	2.4 ± 3.1	0.34
Ischemic TPD, stress-rest (n = 18)	9.2 ± 4.4	10.3 ± 3.8	0.12
Magnitude of stress perfusion deficit (n = 30)	15 ± 9.7*	15.6 ± 8.1	0.5
Magnitude of rest perfusion deficit (n = 18)	3.2 ± 3.5*	3 ± 3.1	0.71
Magnitude of ischemic perfusion deficit (n = 18)	9.2 ± 4.4*	10.5 ± 4.5	0.22

Total perfusion deficit (TPD) and magnitude of perfusion deficit are expressed as mean ± SD. *Comparison of TPD by SPECT-MPI to the magnitude of perfusion deficit quantified on CT-MPI using a semiautomated approach.
  TPD = total perfusion deficit; other abbreviations as in Table 1.

CT-MPI images (Fig. 3). Segments that were abnormal on CT-MPI but normal by SPECT-MPI were often found in the apex, distal LV, or adjacent to segments that were unequivocally abnormal by SPECT-MPI and CT-MPI. In 3 patients, perfusion abnormalities were seen in the basal inferior wall, a region susceptible to beam hardening artifact, on CT-MPI that were not present on SPECT-MPI. On a per-segment basis, the sensitivity, specificity, positive predictive value, and negative predictive value of CT-MPI compared with SPECT were 92%, 86%, 71%, and 96%, respectively.

CT-MPI and SPECT-MPI measurement of stress TPD, rest TPD, and ischemic TPD. There was no significant difference in TPD measured by SPECT-MPI and CT-MPI: p = 0.65 for stress TPD, p = 0.34 for rest TPD, and p = 0.12 for ischemic TPD (Table 2). By Bland-Altman analysis, there was strong simi-

larity between visual assessment of stress TPD by CT-MPI and automated assessment of stress TPD by SPECT-MPI, and there was no significant bias (−0.3) (Fig. 4). Ischemic TPD assessed visually by CT-MPI showed good agreement with automated assessment of SPECT-MPI, with a minimal bias of 1.2 (Fig. 4).

Software-based magnitude of perfusion abnormality measured by CT-MPI compared to TPD by SPECT-MPI. Magnitude of stress perfusion deficit, rest perfusion deficit, and ischemia measured by CT-MPI using commercially available software was similar to that by automated measurement of TPD on SPECT-MPI: p = 0.5 for stress, p = 0.71 for rest, and p = 0.22 for ischemia (Table 2). By Bland-Altman analysis, there was minimal bias, 0.6, when the magnitude of stress perfusion deficit by CT-MPI was compared with that of stress TPD by SPECT-
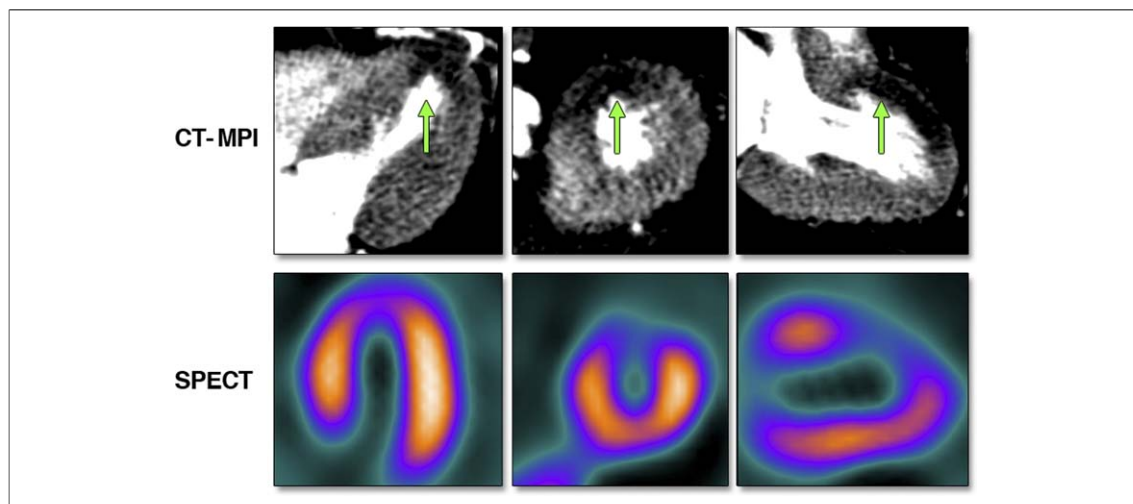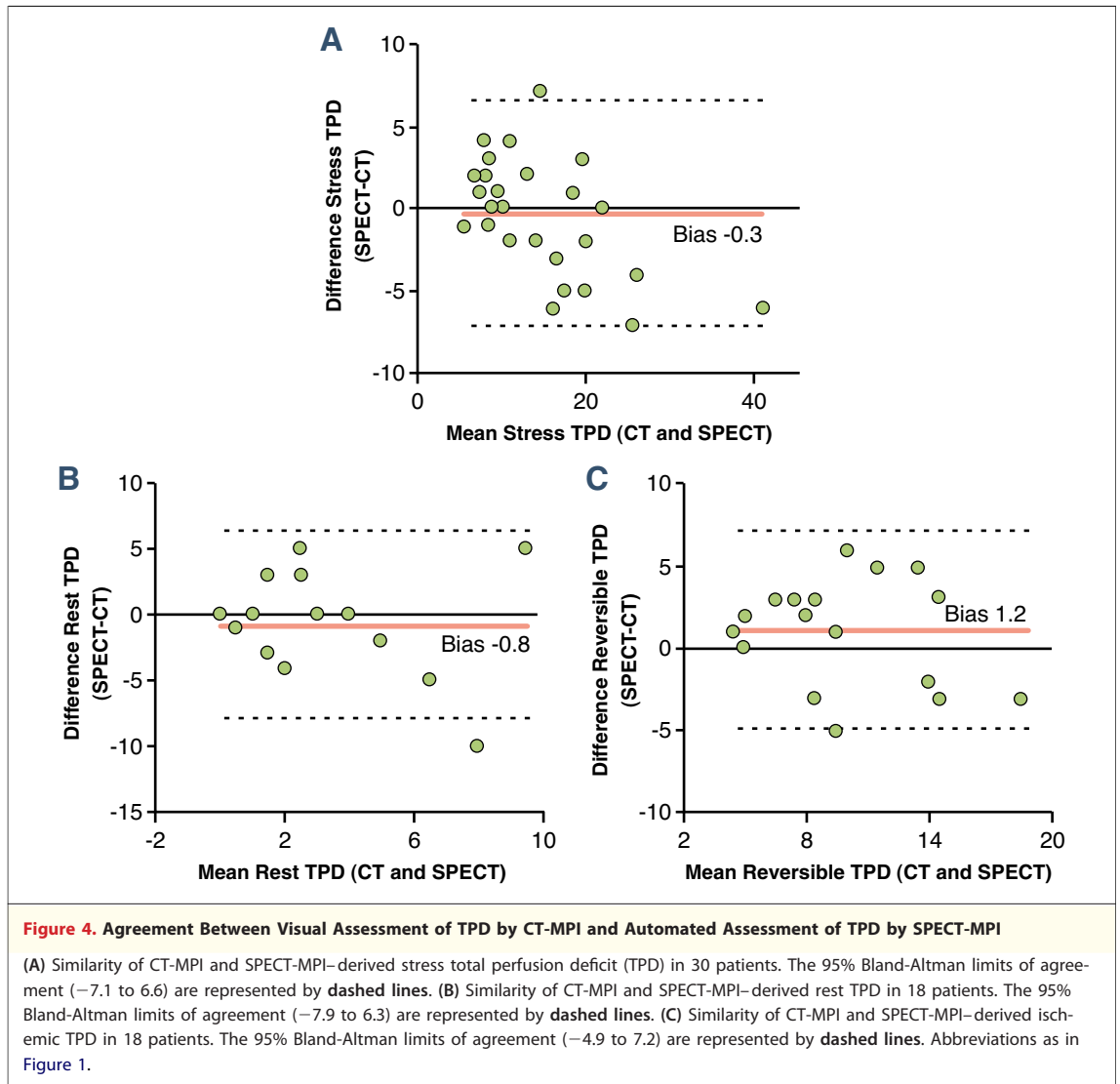

Figure 3. Comparison of Perfusion Defect on CT-MPI and SPECT-MPI

(Top) Stress perfusion defect, indicated by the **green arrows**, in the mid- and distal anterior wall during adenosine stress CT-MPI. **(Bottom)** The perfusion defect in the same wall segments using SPECT-MPI. Abbreviations as in Figure 1.

Figure 4. Agreement Between Visual Assessment of TPD by CT-MPI and Automated Assessment of TPD by SPECT-MPI

(A) Similarity of CT-MPI and SPECT-MPI–derived stress total perfusion deficit (TPD) in 30 patients. The 95% Bland-Altman limits of agreement (−7.1 to 6.6) are represented by **dashed lines**. **(B)** Similarity of CT-MPI and SPECT-MPI–derived rest TPD in 18 patients. The 95% Bland-Altman limits of agreement (−7.9 to 6.3) are represented by **dashed lines**. **(C)** Similarity of CT-MPI and SPECT-MPI–derived ischemic TPD in 18 patients. The 95% Bland-Altman limits of agreement (−4.9 to 7.2) are represented by **dashed lines**. Abbreviations as in Figure 1.
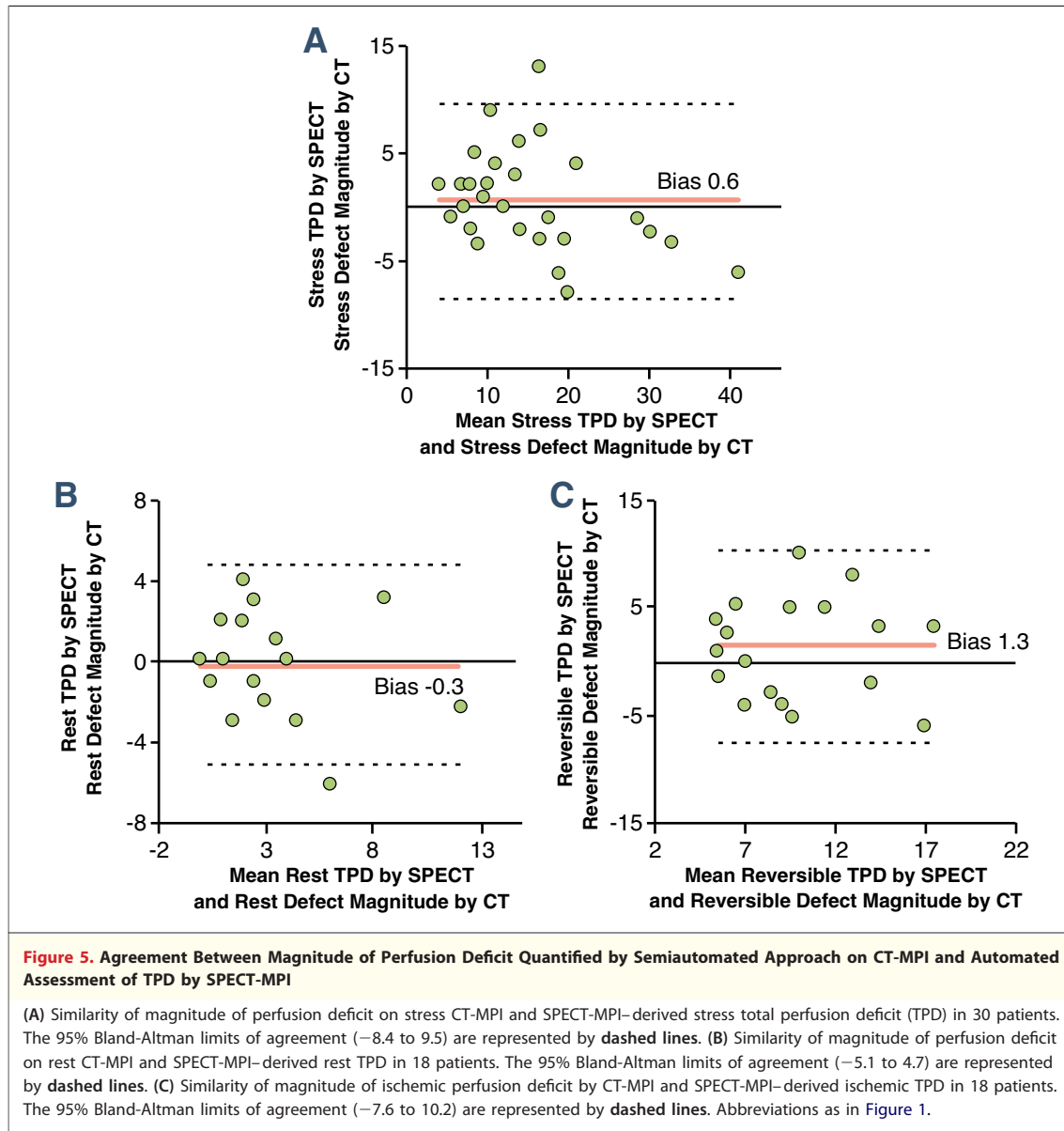
MPI (Fig. 5). By Bland-Altman analysis, the magnitude of ischemia measured by CT-MPI using commercially available software was similar to that of automated measurement of ischemic TPD on SPECT-MPI, with a minimal bias of 1.3 (Fig. 5).

DISCUSSION

SPECT-MPI is an accepted standard for detection and quantification of significant myocardial ischemia and has strong prognostic value for adverse cardiac events (29–31). A fully automated assessment of the extent and severity of myocardial perfusion defects on SPECT-MPI, expressed as TPD, has been validated in previous studies, and the prognostic value of SPECT-MPI–based assessment of stress perfusion defects for the prediction of

future adverse cardiac events is well established (20,29,30). Assessment of the magnitude of ischemia using SPECT-MPI has been shown to predict likelihood of benefit from coronary revascularization in stable ischemic heart disease (18,31,32). To our knowledge, ours is the first study that compares a visual, semiquantitative assessment of the combined extent and severity of myocardial perfusion abnormality by CT-MPI to an automated quantification of perfusion deficit by SPECT-MPI. Our study demonstrates the strong similarity between visual assessment of the extent and severity of perfusion defects by CT-MPI (visual TPD) with an automated assessment of the extent and severity of perfusion defects (TPD) by SPECT-MPI. A recently published study compared SPECT-MPI and CT-MPI stress myocardial perfusion using a 17-

Figure 5. Agreement Between Magnitude of Perfusion Deficit Quantified by Semiautomated Approach on CT-MPI and Automated Assessment of TPD by SPECT-MPI

(A) Similarity of magnitude of perfusion deficit on stress CT-MPI and SPECT-MPI–derived stress total perfusion deficit (TPD) in 30 patients. The 95% Bland-Altman limits of agreement (−8.4 to 9.5) are represented by **dashed lines**. **(B)** Similarity of magnitude of perfusion deficit on rest CT-MPI and SPECT-MPI–derived rest TPD in 18 patients. The 95% Bland-Altman limits of agreement (−5.1 to 4.7) are represented by **dashed lines**. **(C)** Similarity of magnitude of ischemic perfusion deficit by CT-MPI and SPECT-MPI–derived ischemic TPD in 18 patients. The 95% Bland-Altman limits of agreement (−7.6 to 10.2) are represented by **dashed lines**. Abbreviations as in Figure 1.

segment, 3-point visual scale for quantification of abnormal perfusion by CT-MPI, without the use of objective software-based techniques (33). The use of objective automated tools is significant because it removes any possibility of bias in these comparisons. We used a 17-segment, 5-point scale that has been used in prognostic studies to demonstrate the strong association between abnormal SPECT-MPI and adverse cardiac events and is widely used as a standard for clinical assessment of SPECT-MPI (20,24,31,32).

We also show for the first time that a semiautomated assessment of the perfusion deficit by CT-MPI using commercially available software closely matches the perfusion deficit measured using an automated computer-based analysis of SPECT-MPI. Software-based quantification of the magnitude of perfusion deficit by CT-MPI required manually assigned regions with perfusion abnormalities, consensually applied by 2 experienced readers. This measurement is, therefore, tedious and dependent on reader interaction and bias; however, our analysis shows that, despite this limitation, there is minimal bias and strong similarity between this software-based assessment of the magnitude of perfusion deficit on CT-MPI and an automated SPECT-MPI–based assessment of TPD at stress and rest.

On a per-segment basis, compared with SPECT-MPI, CT-MPI shows high sensitivity and a lower specificity for the detection of stress perfu-

sion abnormalities. This finding may be related to the superior spatial resolution of CT-MPI and the improved visualization of the transmural extent of perfusion abnormalities using CT-MPI.

Study limitations. Our investigation included a limited number of subjects, and the extent and severity of perfusion defects on CT-MPI were visually assessed. Qualitatively, rest images were often of better quality than were stress CT-MPI, since beta blockers were used to control heart rate; however, stress CT-MPI images were of diagnostic quality with our dual-source CT scanner, even with slightly higher heart rates. Compared to other studies reported in the literature, our effective radiation dose was considerably higher (10–13). That higher dose was in part due to the inclusion of patients who had coronary artery bypass graft surgery, which required greater scan length (22 cm to 11cm, median 18 cm) for visualization of the aortic arch and the internal mammary artery. In the future, with new-generation scanners and aggressive dose modulation, an effective radiation dose comparable to that for SPECT-MPI may be achieved for CT-MPI. We did not have invasive coronary angiography data to verify the use of SPECT-MPI as a reference; however, our primary goal was to compare the assessment of ischemia by CT-MPI to that by SPECT-MPI. Automated software for comparison of normal and abnormal patterns of myocardial contrast distribution for the identification of true perfusion defects has not been developed. Such tools for objective identification of perfusion defects are needed to distinguish truly abnormal myocardium from segments of "normal" myocardium on CT-MPI that might have appeared hypoperfused because of variations in contrast distribution. Future studies involving larger numbers of patients will be necessary for the validation of our findings.

CONCLUSIONS

Myocardial perfusion measured by CT-MPI shows strong similarity to that obtained by SPECT-MPI, suggesting that CT-MPI–based assessment of myocardial perfusion defects has the potential to be of similar clinical and prognostic value for prediction of future cardiovascular risk.

Reprint requests and correspondence: Dr. Daniel S. Berman, Department of Imaging, Cedars-Sinai Medical Center, 8700 Beverly Boulevard, Room 1258, Los Angeles, California 90048. *E-mail:* bermand@cshs.org.

REFERENCES

1. Mowatt G, Cook JA, Hillis GS, et al. 64-Slice computed tomography angiography in the diagnosis and assessment of coronary artery disease: systematic review and meta-analysis. Heart 2008;94:1386–93.

2. Budoff MJ, Dowe D, Jollis JG, et al. Diagnostic performance of 64-multidetector row coronary computed tomographic angiography for evaluation of coronary artery stenosis in individuals without known coronary artery disease: results from the prospective multicenter ACCURACY (Assessment by Coronary Computed Tomographic Angiography of Individuals Undergoing Invasive Coronary Angiography) trial. J Am Coll Cardiol 2008;52:1724–32.

3. Meijboom WB, Meijs MF, Schuijf JD, et al. Diagnostic accuracy of 64-slice computed tomography coronary angiography: a prospective, multi-center, multivendor study. J Am Coll Cardiol 2008;52:2135–44.

4. Miller JM, Rochitte CE, Dewey M, et al. Diagnostic performance of coronary angiography by 64-row CT. N Engl J Med 2008;359:2324–36.

5. Schuijf JD, Wijns W, Jukema JW, et al. Relationship between noninvasive coronary angiography with multi-slice computed tomography and myocardial perfusion imaging. J Am Coll Cardiol 2006;48:2508–14.

6. Gaemperli O, Schepis T, Koepfli P, et al. Accuracy of 64-slice CT angiography for the detection of functionally relevant coronary stenoses as assessed with myocardial perfusion SPECT. Eur J Nucl Med Mol Imaging 2007;34:1162–71.

7. Sato A, Hiroe M, Tamura M, et al. Quantitative measures of coronary stenosis severity by 64-slice CT angiography and relation to physiologic significance of perfusion in nonobese patients: comparison with stress myocardial perfusion imaging. J Nucl Med 2008;49:564–72.

8. George RT, Silva C, Cordeiro MA, et al. Multidetector computed tomography myocardial perfusion imaging during adenosine stress. J Am Coll Cardiol 2006;48:153–60.

9. George RT, Jerosch-Herold M, Silva C, et al. Quantification of myocardial perfusion using dynamic 64-detector computed tomography. Invest Radiol 2007;42:815–22.

10. Ruzsics B, Lee H, Zwerner PL, Gebregziabher M, Costello P, Scho-epf UJ. Dual-energy CT of the heart for diagnosing coronary artery stenosis and myocardial ischemia-initial experience. Eur Radiol 2008;18:2414–24.

11. George RT, Arbab-Zadeh A, Miller JM, et al. Adenosine stress 64- and 256-row detector computed tomography angiography and perfusion imaging: a pilot study evaluating the transmural extent of perfusion abnormalities to predict atherosclerosis causing myocardial ischemia. Circ Cardiovasc Imaging 2009;21:74–82.

12. Blankstein R, Shturman LD, Rogers IS, et al. Adenosine-induced stress myocardial perfusion imaging using dual-source cardiac computed tomography. J Am Coll Cardiol 2009;54:1072–84.

13. Ruzsics B, Schwarz F, Schoepf UJ, et al. Comparison of dual-energy computed tomography of the heart with single photon emission computed tomography for assessment of coronary artery stenosis and of the myocardial blood supply. Am J Cardiol 2009;104:318–26.

14. Flohr TG, McCollough CH, Bruder H, et al. First performance evaluation of a dual-source CT (DSCT) system. Eur Radiol 2006;16:256–68.

15. Dey D, Lee CJ, Ohba M, et al. Image quality and artifacts in coronary CT angiography with dual-source CT: initial clinical experience. J Cardiovasc Comput Tomogr 2008;2:105–14.

16. Gutstein A, Dey D, Cheng V, et al. Algorithm for radiation dose reduction with helical dual source coronary computed tomography angiography in clinical practice. J Cardiovasc Comput Tomogr 2008;2:311–22.

17. Hausleiter J, Meyer T, Hermann F, et al. Estimated radiation dose associated with cardiac CT angiography JAMA 2009;301:500–7.

18. Blankstein R, Okada DR, Rocha-Filho JA, Rybicki FJ, Brady TJ, Cury R. Cardiac myocardial perfusion imaging using dual source computed tomography. Int J Card Imaging 2009; 25:209–16.

19. Hachamovitch R, Hayes SW, Friedman JD, Cohen I, Berman DS. Comparison of the short-term survival benefit associated with revascularization compared with medical therapy in patients with no prior coronary artery disease undergoing stress myocardial perfusion single photon emission computed tomography. Circulation 2003;107:2900–7.

20. Berman DS, Abidov A, Kang X, et al. Prognostic validation of a 17-segment score derived from a 20-segment score for myocardial perfusion SPECT interpretation. J Nucl Cardiol 2004;11:414–23.

21. Berman DS, Kang X, Hayes SW, et al. Adenosine myocardial perfusion single-photon emission computed tomography in women compared with men. Impact of diabetes mellitus on incremental prognostic value and ef-

fect on patient management. J Am Coll Cardiol 2003;41:1125–33.

22. Nishina H, Slomka PJ, Abidov A, et al. Combined supine and prone quantitative myocardial perfusion SPECT: method development and clinical validation in patients with no known coronary artery disease. J Nucl Med 2006;47:51–8.

23. Germano G, Kavanagh PB, Su HT, et al. Automatic reorientation of three-dimensional, transaxial myocardial perfusion SPECT images. J Nucl Med 1995;36:1107–14.

24. Slomka PJ, Nishina H, Berman DS, et al. Automated quantification of myocardial perfusion SPECT using simplified normal limits. J Nucl Cardiol 2005;12:66–77.

25. Berman DS, Kang X, Gransar H, et al. Quantitative assessment of myocardial perfusion abnormality on SPECT myocardial perfusion imaging is more reproducible than expert visual analysis. J Nucl Cardiol 2009;16:45–53.

26. Slomka PJ, Cheng VY, Dey D, et al. Quantitative analysis of myocardial perfusion SPECT anatomically guided by coregistered 64-slice coronary CT angiography. J Nucl Med 2009;50:1621–30.

27. Cohen J. A coefficient of agreement for nominal scales. Educ Psycholog Measure 1960;20:37–46.

28. Bland JM, Altman DG. Statistical methods for assessing agreement between two methods of clinical measurement. Lancet 1986;1:307–10.

29. Hachamovitch R, Berman DS, Kiat H, et al. Exercise myocardial perfusion SPECT in patients without

known coronary artery disease: incremental prognostic value and use in risk stratification. Circulation 1996; 93:905–14.

30. Hachamovitch R, Berman DS, Shaw LJ, et al. Incremental prognostic value of myocardial perfusion single photon emission computed tomography for the prediction of cardiac death: differential stratification for risk of cardiac death and myocardial infarction. Circulation 1998;97:535–43.

31. Shaw LJ, Berman DS, Maron DJ, et al. Optimal medical therapy with or without percutaneous coronary intervention to reduce ischemic burden: results from the Clinical Outcomes Utilizing Revascularization and Aggressive Drug Evaluation (COURAGE) trial nuclear substudy. Circulation 2008;17:1283–91.

32. Hachamovitch R, Kang X, Amanullah AM, et al. Prognostic implications of myocardial perfusion single-photon emission computed tomography in the elderly. Circulation 2009;20:2197–206.

33. Okada DR, Ghoshhajra BB, Blankstein R, et al. Direct comparison of rest and adenosine stress myocardial perfusion CT with rest and stress SPECT. J Nucl Cardiol 2009;17: 27–37.

Key Words: computed tomography ▪ ischemia ▪ myocardial perfusion imaging ▪ single photon emission computed tomography.